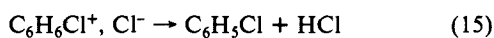
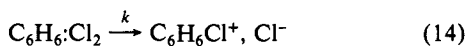
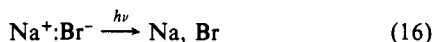


Other reactions of the complexes do have rates that correlate with ν_{\max} . In a series of examples, Fukuzumi and Kochi²⁵ have shown that electrophilic substitution shows a good correlation between rate constants ($\log k$) and ν_{\max} for a series of substituted benzenes and of olefins. Taking chlorination as an example, the mechanism is



In this case the charge-transfer transition (12) is just the one needed to drive the rate-determining step (14).

Any Lewis acid–base reaction can be considered to lead to a charge-transfer complex, with partial transfer of electrons from the base to the acid. The molecule NaBr can be considered as formed from Na^+ and Br^- . In such cases the ground state is very ionic, and the excited state is covalent. Accordingly, the



charge-transfer band is the transition that drives the reaction, since the gas-phase dissociation will be to the neutral atoms. This accounts for the good linearity shown in Figure 2.

(25) Fukuzumi, S.; Kochi, J. K. *J. Am. Chem. Soc.* **1981**, *103*, 7240–7252; **1982**, *104*, 7599–7609.

Charge-transfer bonds are usually very intense, since they are fully allowed and have a high transition moment. Even if ν_{\max} is in the UV, there can be a long tail that extends into the visible and gives rise to color. This is the case with the permanganate ion, where ν_{\max} in water is actually 52.9 kK, well into the ultraviolet. The bond is a ligand-to-metal charge-transfer transition.

Summary. Even if only the first absorption band is considered, there is evidently a great deal of chemical information in the electronic spectra of molecules. However, it is usually necessary to use spectroscopic theory to identify the nature of the first band. In most cases only elementary theory is needed. It is also necessary to compare families of molecules that are closely related in some way.

A large value of ν_{\max} is a reliable indication of high kinetic stability. Conversely, a colored molecule is very likely to show high reactivity,²⁶ but only for reactions consistent with the nature of the transition.

Acknowledgment. This work was supported by a grant from the U.S. Department of Energy (Contract No. DE AS03-76SF00034).

(26) Especially small molecules. A large delocalized molecule might have the activating effect of the first transition widely diffused over many atoms. An example would be the dyes based on triphenylmethane.

(27) Rosenstock, H. M.; Draxl, K.; Steiner, B. W.; Herron, J. T. *J. Phys. Chem. Ref. Data* **1977**, *6*, Suppl. No. 1.

(28) McMillen, D. F.; Golden, D. M. *Annu. Rev. Phys. Chem.* **1982**, *33*, 493–532.

Recombination of $\text{Cr}(\text{CO})_n$ with CO: Kinetics and Bond Dissociation Energies

T. Rick Fletcher[†] and Robert N. Rosenfeld^{*†}

Contribution from the Department of Chemistry, University of California, Davis, California 95616. Received August 3, 1987

Abstract: The pressure dependence of the recombination kinetics of $\text{Cr}(\text{CO})_5$ and $\text{Cr}(\text{CO})_4$ with CO has been studied with the technique of time-resolved infrared laser absorption spectroscopy. The high pressure limiting rate constants are 2.1×10^6 and $7.5 \times 10^6 \text{ Torr}^{-1} \text{ s}^{-1}$ for $\text{Cr}(\text{CO})_5$ and $\text{Cr}(\text{CO})_4$, respectively. The rate at which vibrationally excited metal carbonyls, $[\text{Cr}(\text{CO})_n]^*$, are collisionally stabilized has been estimated: $k_s = 2.6 \times 10^5$ and $2.5 \times 10^7 \text{ Torr}^{-1} \text{ s}^{-1}$ for collisions with He and $\text{Cr}(\text{CO})_6$, respectively. These data, in conjunction with an RRKM model for the unimolecular decay of $\text{Cr}(\text{CO})_6$ and $\text{Cr}(\text{CO})_5$, allow us to determine the metal–ligand bond dissociation energies; $\text{DH}^\circ[(\text{CO})_5\text{Cr}-\text{CO}] = 37 \pm 5 \text{ kcal/mol}$ and $\text{DH}^\circ[(\text{CO})_4\text{Cr}-\text{CO}] = 25 \pm 5 \text{ kcal/mol}$.

Time-resolved infrared absorption spectroscopy has recently been applied in characterizing the chemistry of a variety of organometallic species in the gas phase.^{1–4} Such studies can provide useful data on dissociation dynamics, primary photochemical channels, reactive intermediate structure, and lifetimes for bimolecular reactions. Information of this type, while valuable in and of itself, is essential in developing mechanistic models for processes, e.g., homogeneous catalysis, where coordinatively unsaturated metal centers may be involved.⁵ Perhaps the seemingly most simple question that can be formulated to this end is the following: How do the decomposition products of a photochemically activated organometallic reagent, $\text{M}(\text{CO})_n^*$, depend on excitation wavelength? The answer to this question apparently depends on experimental conditions. Condensed-phase photolyses characteristically yield products derived from cleavage of a single metal–CO bond, regardless of excitation wavelength.⁶ More

extensive fragmentation may be observed in gas-phase experiments.⁷ How do solvent molecules attenuate reactivity in this way? A priori, one might suggest that efficient collisional relaxation of vibrational and/or electronic energy may serve to (partially) quench reactivity in condensed phases relative to the gas phase. The evaluation of questions such as those posed above requires data on the photophysics, primary photochemistry, and thermochemistry (i.e., bond dissociation energies) of organo-

(1) Poliakoff, M.; Weitz, E. *Adv. Organomet. Chem.* **1986**, *25*, 277.

(2) Weiller, B. H.; Grant, E. R. *J. Am. Chem. Soc.* **1987**, *109*, 1051.

(3) Fletcher, T. R.; Rosenfeld, R. N. *J. Am. Chem. Soc.* **1985**, *107*, 2203.

(4) Rayner, D. M.; Nazran, A. S.; Drouin, M.; Hackett, P. A. *J. Phys. Chem.* **1986**, *90*, 2882.

(5) Whetten, R. L.; Fu, K.-J.; Grant, E. R. *J. Am. Chem. Soc.* **1982**, *104*, 4270.

(6) Geoffroy, G. L.; Wrighton, M. S. *Organometallic Photochemistry*; Academic: New York, 1979.

(7) Tumas, W.; Gitlin, B.; rosan, A. M.; Yardley, J. T. *J. Am. Chem. Soc.* **1982**, *104*, 55.

[†] Present address: JILA, University of Colorado, Boulder, CO 80309.

^{*} A. P. Sloan Fellow, 1985–1987.

metallic compounds. In this article, we outline a procedure for obtaining such thermochemical data.

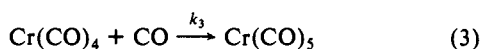
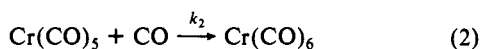
Currently, only limited thermochemical data are available for organometallic compounds. In particular few direct measurements of bond dissociation energies, BDEs, for such species have been reported. This can be contrasted with the case of organic compounds, where extensive tabulations of BDEs exist. Heats of formation for some organo-transition-metal compounds are available,⁸ but data on coordinatively unsaturated metallic species have been especially lacking. The situation is somewhat better for organometallic ions where ion beam,⁹ ion cyclotron resonance,¹⁰ and mass spectrometric¹¹ methods have yielded abundant information on metal-ligand bond strengths. The application of these data in predicting BDEs for *neutral* organometallics requires the availability of additional data, i.e., ionization potentials and/or electron affinities. The necessary data are not generally accessible.

Recently, some new experimental approaches to the measurement of organometallic BDEs have been reported. Peters and co-workers¹² have used the technique of photoacoustic calorimetry to measure the first BDE of some species, $M(CO)_6$, in solution. Lewis et al.¹³ have used laser powered homogeneous pyrolysis to investigate the BDEs of a variety of metal carbonyls in the gas phase. Lineberger and co-workers^{14,15} have used photoelectron spectroscopy to determine the electron affinities of some species, $M(CO)_n^-$, which, when coupled with available appearance potential data, yield BDEs for the corresponding neutrals. In the absence of directly measured BDEs, some workers have defined an average bond energy, $\overline{DH}^\circ(M-CO) = \Delta H_1/n$, eq 1, which is used as an approximation to the individual BDEs. The data of



Lineberger and co-workers^{14,15} clearly demonstrate that this is an inappropriate approximation and that individually measured BDEs must be used.

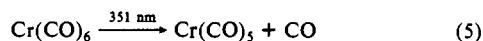
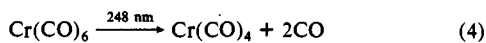
Here, we report kinetic data on the recombination reactions (reactions 2 and 3) (see also ref 3, 16, and 17). In addition, we



discuss the application of unimolecular rate theory in modelling the pressure dependences of these reactions. Comparisons of model with experimental data allow us to estimate the BDE of both $Cr(CO)_6$ and $Cr(CO)_5$. This approach to estimating BDEs appears quite general and should be an especially useful method in the case of coordinatively unsaturated compounds, where more conventional techniques are of limited utility.

Experimental Section

Most of the instrumentation and procedures used in these studies have been previously described in detail,³ so only a brief outline is given here. $Cr(CO)_n$ ($n = 4, 5$) is generated by the pulsed ultraviolet laser photolysis of $Cr(CO)_6$ and detected by time-resolved infrared (IR) spectroscopy by using a continuous wave (CW) CO laser as the IR source. $Cr(CO)_4$ is produced by the KrF* (248 nm) photolysis of $Cr(CO)_6$ while photolysis at 351 nm (XeF* laser) yields $Cr(CO)_5$, eq 4 and 5, respectively.



(8) Conner, J. A. *Top. Current Chem.* **1977**, *71*, 71.

(9) Georgiadis, R.; Armentrout, P. B. *J. Am. Chem. Soc.* **1986**, *108*, 2119.

(10) Hettich, R. L.; Freiser, B. S. *J. Am. Chem. Soc.* **1986**, *108*, 2537.

(11) Saalfeld, F. E.; McDowell, M. V.; DeCoppo, J. J.; Berry, A. D.; MacDiarmid, A. G. *Inorg. Chem.* **1973**, *12*, 48.

(12) Bernstein, M.; Simon, J. D.; Peters, K. S. *Chem. Phys. Lett.* **1983**, *100*, 241.

(13) Lewis, K. E.; Golden, D. M.; Smith, G. P. *J. Am. Chem. Soc.* **1984**, *106*, 3905.

(14) Engelking, P. C.; Lineberger, W. C. *J. Am. Chem. Soc.* **1979**, *101*, 5569.

(15) Stevens, A. E.; Feigerle, C. S.; Lineberger, W. C. *J. Am. Chem. Soc.* **1982**, *104*, 5026.

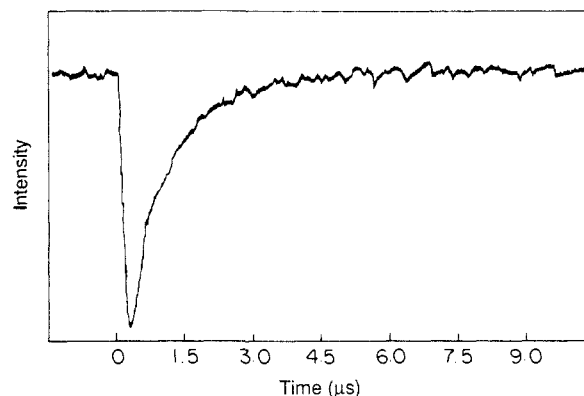


Figure 1. Time-resolved absorption due to $Cr(CO)_4$ at 1915 cm^{-1} , corresponding to $\nu_{CO}(b_2)$, following the 248-nm photolysis of $Cr(CO)_6$. Experimental conditions are the following: $[Cr(CO)_6] = 0.020 \text{ Torr}$, $[CO] = 0.400 \text{ Torr}$, and $[He] = 80.0 \text{ Torr}$.

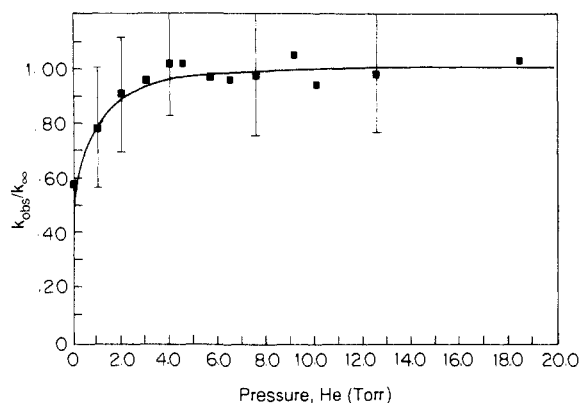


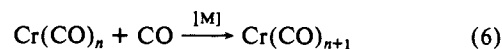
Figure 2. Pressure dependence of the rate constant for the recombination of $Cr(CO)_5$ with CO. The solid line corresponds to an RRKM calculation where $E_0 = 37 \text{ kcal/mol}$. See text.

Identities of the photoproducts are determined by time-resolved IR laser absorption spectroscopy, as previously described.^{3,16} Samples generally consist of $Cr(CO)_6$ [0.010 Torr], He [0–80 Torr], and CO [0.040–5.00 Torr] housed in a 100-cm Pyrex cell equipped with CaF_2 windows. The time-dependent concentration of $Cr(CO)_4$ is monitored at 1915 cm^{-1} [$\nu_{CO}(b_2)$] or 1948 cm^{-1} [$\nu_{CO}(b_1)$] while that for $Cr(CO)_5$ is monitored at 1987 cm^{-1} [$\nu_{CO}(e)$]. The time constant of the detection system is ca. 200 ns. Both $Cr(CO)_5$ and $Cr(CO)_4$ are formed within 200 ns of the photolysis of $Cr(CO)_6$ and both are characterized by simple exponential decays for at least 2.5 half-lives under high-pressure conditions (total pressure in excess of 20 Torr). For lower pressures, it was sometimes necessary to use two exponentials to fit the decay data (vide infra).

Infrared fluorescence experiments were carried out as previously described,^{18,19} using a 50-mm² InSb detector. A narrow band-pass filter ($1900 \pm 70 \text{ cm}^{-1}$) was used to isolate emission due to $Cr(CO)_4$. This filter blocks at least 98% of any IR emission from the CO photoproduct. The time constant of the detection system employed for fluorescence experiments was ca. 1 μs .

Results and Discussion

The kinetics of the recombination reactions (eq 2 and 3) were determined by generating $Cr(CO)_n$ [$n = 4, 5$] in the presence of CO and He and then monitoring the relative concentration of $Cr(CO)_n$ or $Cr(CO)_{n+1}$ as a function of time. See Figure 1. Rate



constants, k_2 and k_3 , can be determined either by dividing the signal decay rate by the CO pressure, $[CO]$, or by plotting the

(16) Fletcher, T. R.; Rosenfeld, R. N. *High Energy Processes in Organometallic Chemistry*, Suslick, K. S., Ed.; American Chemical Society: Washington, DC, 1987; ACS Symp. Ser. 333, pp 99.

(17) Seder, T. A.; Church, S. P.; Weitz, E. J. *Am. Chem. Soc.* **1986**, *108*, 4721.

(18) Rosenfeld, R. N.; Weiner, B. J. *Am. Chem. Soc.* **1983**, *105*, 3485.

(19) Sonobe, B. I.; Rosenfeld, R. N. *J. Am. Chem. Soc.* **1983**, *105*, 7528.

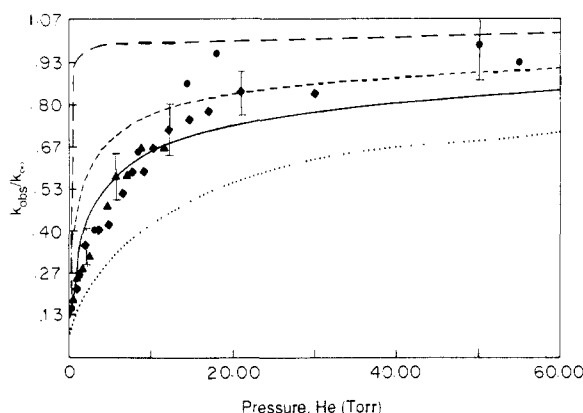
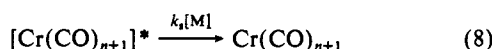
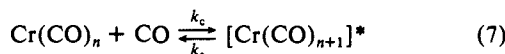


Figure 3. Pressure dependence of the rate constant for the recombination of Cr(CO)₄ with CO. Lines correspond to RRKM calculations where (---) $E_0 = 40$, (-.-) $E_0 = 25$, (—) $E_0 = 23$, and (···) $E_0 = 20$ kcal/mol. See text. The various symbols correspond to rate constants measured at different laser frequencies.

decay rate versus [CO] and taking the slope of the best straight line through the data. The two methods gave identical results within experimental uncertainty so the latter was normally used only as a means of checking the former. We find that the apparent rate constants, k_2 and k_3 , increase with increasing [M] (M = He or Ar) and approach limiting high-pressure values. See Figures 2 and 3. For (2), the high-pressure limiting rate constant is $k_2^\infty = 2.1 \pm 0.5 \times 10^6 \text{ Torr}^{-1} \text{ s}^{-1}$, while for (3), we find $k_3^\infty = 7.5 \pm 1.3 \times 10^6 \text{ Torr}^{-1} \text{ s}^{-1}$, where the indicated uncertainties represent $\pm 2\sigma$.

The pressure dependences of k_2 and k_3 can be qualitatively explained in terms of a Lindemann-type recombination mechanism (eq 7 and 8), where the asterisk indicates ro-vibrational excitation



and $n = 4$ or 5 . This mechanism has a simple physical interpretation. The species initially formed by recombination, $[\text{Cr}(\text{CO})_{n+1}]^*$, is chemically activated, i.e., it contains an amount of internal energy, ca. $\text{DH}^\circ[(\text{CO})_n\text{Cr}-\text{CO}]$, sufficient for decomposition back to reactants, $\text{Cr}(\text{CO})_n + \text{CO}$. Thus, $[\text{Cr}(\text{CO})_{n+1}]^*$ will dissociate unless at least some of this internal energy is removed by collisions with the bath gas, [M]. The overall rate constant for $\text{Cr}(\text{CO})_n$ decay or $\text{Cr}(\text{CO})_{n+1}$ formation depends on the relative values of k_c and $k_s[\text{M}]$. If the steady state approximation, $d[\text{Cr}(\text{CO})_{n+1}]^*/dt = 0$, is made, one obtains an expression for this overall rate constant, k_{obsd} , eq 9. Here, $k_s[\text{M}]$ has been replaced by $\sum k_s[\text{M}]$ to account for the several third bodies, M,

$$k_{\text{obsd}} = k_c \sum k_s[\text{M}] / (k_a + \sum k_s[\text{M}]) \quad (9)$$

present, i.e., eq 10. The expression for k_{obsd} , eq 9, has two simple

$$\sum k_s[\text{M}] = k_s^{(1)}[\text{He}] + k_s^{(2)}[\text{CO}] + k_s^{(3)}[\text{Cr}(\text{CO})_6] \quad (10)$$

limiting forms, the high- and low-pressure limits, given by (11) and (12), respectively. Thus, k_c can be determined directly from the measured k_{obsd}^∞ . We will show below how $\sum k_s[\text{M}]$ can be

$$k_{\text{obsd}}^\infty = \lim_{[\text{M}] \rightarrow \infty} (k_{\text{obsd}}) = k_c \quad (11)$$

$$k_{\text{obsd}}^0 = \lim_{[\text{M}] \rightarrow 0} (k_{\text{obsd}}) = (k_c/k_a) \sum k_s[\text{M}] \quad (12)$$

independently estimated from experimental data so that k_a is the only unknown quantity in eq 9. If some physical model permits k_a to be calculated and k_a is known to be a function of a parameter, x , i.e., $k_a = k_a(x)$, then (9) can be evaluated for various choices of x . By comparing calculations with experimental data, the value of x can thereby be determined. Because k_a is the rate constant for the unimolecular decomposition of $[\text{Cr}(\text{CO})_{n+1}]^*$, it can be computed with RRKM theory.^{20,21}

Table I. Input Parameters for RRKM Calculations: $\text{Cr}(\text{CO})_6 \rightarrow \text{Cr}(\text{CO})_5 + \text{CO}$ (Degeneracies Indicated in Parentheses)

	reactant Cr(CO) ₆	transition state (CO) ₅ Cr...CO
vibrational freq (cm ⁻¹)	2118 (1) 2026 (2) 2000 (3) 668 (3) 532 (3) 510 (3) 440 (3) 390 (2) 379 (1) 364 (3) 97 (3) 89 (3) 67 (3)	2143 (1) 2026 (2) 2000 (3) 668 (3) 532 (3) 510 (1) 440 (2) 390 (2) 379 (1) 364 (3) 175 (2) 97 (3) 89 (1) 67 (3) 50 (3)
moments of inertia (amu·Å ²)	775.46 (3)	1686.61 (2) 775.46 (1)
reaction path degeneracy		$L^* = 6$

RRKM theory has found extensive application in modeling the dissociation kinetics of chemically activated species. Using this formalism, we can express k_{obsd} as in eq 13, where the energy

$$k_{\text{obsd}} = \int_0^\infty \frac{k_c \sum k_s[\text{M}]}{k_a(E) + \sum k_s[\text{M}]} F(E) dE \quad (13)$$

dependence of k_a is explicitly indicated and $F(E)$ is a function describing the distribution of energized molecules. The RRKM expression for $k_a(E)$ is given by²⁰ (14), where L^* is the reaction

$$k_a(E) = L(Q_1^+/Q) [hN(E)]^{-1} \sum_{E^+_{vr}=0}^{E-E_0} P(E^+_{vr}) \quad (14)$$

path degeneracy, (Q_1^+/Q) is the ratio of transition state and reactant adiabatic rotational partition functions, $N(E)$ is the density of states of the reactant with internal energy, E , $P(E^+_{vr})$ is the number of transition states at internal energy, E^+_{vr} , and E_0 is the critical energy for the unimolecular decomposition reaction. The distribution function, $F(E)$, is given²¹ by eq 15, where the

$$F(E) = \frac{G(E - E_0) e^{-E/kT}}{\int_0^\infty G(E - E_0) e^{-E/kT} dE} \quad (15)$$

sum of states for the transition state is $G(E - E_0) = \sum_{E^+_{vr}=0}^{E-E_0} P(E^+_{vr})$. $k_a(E)$ and $F(E)$ are evaluated by using the Whitten-Rabinovitch algorithm²² to estimate sums and densities of states in (14) and (15). The integrand in (13) is numerically integrated to obtain k_{obsd} . By repeating this process for various values of [M], the pressure dependence of k_{obsd} can be calculated. $N(E)$ depends on the vibrational frequencies and moments of inertia of the reactant, $[\text{Cr}(\text{CO})_{n+1}]^*$. $G(E - E_0)$ depends on analogous quantities for the transition state and also on the value selected for E_0 . If the reactants' and transition state's vibrational frequencies and moments of inertia can be estimated, then $k_a(E)$ is determined by the choice of E_0 . Thus, the pressure dependence of k_{obsd} , eq 9, can be calculated for various choices of E_0 and compared with the measured pressure dependence to find the best choice of E_0 .

The parameters used in calculating $k_a(E)$ for $\text{Cr}(\text{CO})_6$ and $\text{Cr}(\text{CO})_5$ are listed in Tables I and II, respectively. Vibrational frequencies for $\text{Cr}(\text{CO})_5$ were assumed to be identical with those for $\text{Cr}(\text{CO})_6$ after allowing for the reduction in the number of vibrational modes in the former case. A comparison with several

(20) Robinson, P. J.; Holbrook, K. A. *Unimolecular Reactions*; Wiley-Interscience: New York, 1972.

(21) Forst, W. *Theory of Unimolecular Reactions*; Academic: New York, 1973.

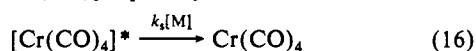
(22) Whitten, G. Z.; Rabinovitch, B. S. *J. Chem. Phys.* 1964, 41, 1883.

Table II. Input Parameters for RRKM Calculations: $\text{Cr}(\text{CO})_5 \rightarrow \text{Cr}(\text{CO})_4 + \text{CO}$ (Degeneracies Indicated in Parentheses)

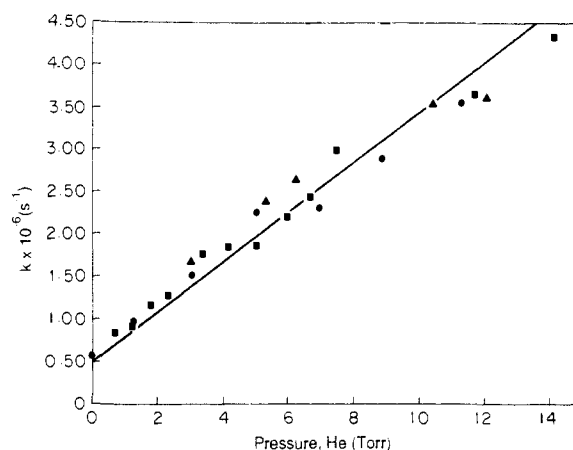
	reactant $\text{Cr}(\text{CO})_5$	transition state $\text{Cr}(\text{CO})_4 \cdots \text{CO}$
vibrational freq (cm^{-1})	2066 (2) 2000 (3) 668 (1) 532 (3) 510 (3) 440 (2) 390 (2) 379 (1) 364 (3) 97 (1) 89 (3) 67 (3)	2143 (1) 2026 (2) 2000 (2) 558 (1) 532 (3) 510 (1) 440 (1) 390 (2) 379 (1) 364 (3) 175 (2) 97 (1) 89 (1) 67 (3) 50 (2)
moments of inertia ($\text{amu}\cdot\text{\AA}^2$)	775.46 (1) 554.62 (2)	1504.60 (1) 1282.53 (1) 553.38 (1)
reaction path degeneracy		$L^* = 4$

model compounds [e.g., $\text{Ni}(\text{CO})_4$, $\text{Fe}(\text{CO})_5$, $\text{Mn}(\text{CO})_5\text{Cl}$, ...] indicates that the frequencies of the M—C and C=O stretching vibrations and the various bending vibrations are similar from compound to compound.²³ Transition-state parameters were determined as follows. The high-pressure Arrhenius pre-exponential factors, A_{∞} , for the thermal decomposition of several metal carbonyls have been measured and are comparable,¹³ i.e., for $\text{Fe}(\text{CO})_5$, $\text{Mo}(\text{CO})_6$, and $\text{W}(\text{CO})_6$, $A_{\infty} = 10^{15.8}$, $10^{15.6}$, and $10^{15.6}$ s^{-1} , respectively. We thus assume that both $\text{Cr}(\text{CO})_6$ and $\text{Cr}(\text{CO})_5$ dissociate via "loose" transition states. The interfragment separation at the transition state, r^* [$(\text{CO})_n\text{Cr}\cdots\text{CO}$], can then be calculated by the method of Waage and Rabinovitch.²⁴ We find $r^* \sim 5.2$ Å. Under these conditions, the transition state's vibrational frequencies can be approximated by those of the isolated fragments, $\text{Cr}(\text{CO})_n$ and CO. Internal rotation in the transition state is then hindered as necessary (ca. 90%) to reproduce the experimental (or estimated) value of ΔS^* (ca. 9.9 eu). Troe and co-workers²⁵ have shown that the value of $k_a(E)$ calculated via (14) is generally insensitive to the values of the transition-state vibrational frequencies used so long as the frequencies and moments of inertia chosen yield the correct value of ΔS^* . We have confirmed this by noting that if the frequencies used for $\text{Cr}(\text{CO})_5$ (Table I) are replaced by those²³ of $\text{Fe}(\text{CO})_5$, the calculated fall-off curve (k_{obsd} versus pressure) changes by less than 10%, so long as $\Delta S^* = 9.9$ eu is maintained. If we assume the reactant and transition-state parameters for the decomposition of $\text{Cr}(\text{CO})_6$ and $\text{Cr}(\text{CO})_5$ to be fixed (Tables I and II), then $k_a(E)$ depends only on the choice of E_0 , within the framework of an RRKM model.

The evaluation of eq 9 requires that $\sum k_s[\text{M}]$ be determined. Ideally, one would like to measure the rate constants, k_s , with which both $[\text{Cr}(\text{CO})_6]^*$ and $[\text{Cr}(\text{CO})_5]^*$ are deactivated via collisions with He, CO, and $\text{Cr}(\text{CO})_6$. Experimental difficulties have, to date, precluded such measurements (vide infra), but analogous data on the deactivation of $[\text{Cr}(\text{CO})_4]^*$, eq 16, can be obtained. When $\text{Cr}(\text{CO})_6$ is photolyzed at 248 nm, the nascent



$\text{Cr}(\text{CO})_4$ product is vibrationally excited. Two independent experiments provide evidence for this. Following photolysis, infrared fluorescence near 1900 cm^{-1} is observed. Filter studies indicate this emission originates from the $\nu_{\text{CO}}(\text{b}_2)$ mode of $\text{Cr}(\text{CO})_4$. The fluorescence decay rate increases with increasing helium pressure, [He]. Additionally, the time-resolved IR spectrum of $\text{Cr}(\text{CO})_4$

**Figure 4.** Pressure dependence of the $[\text{Cr}(\text{CO})_4]^*$ decay rate. $[\text{Cr}(\text{CO})_6] = 0.02$ Torr. The solid line is a linear least-squares fit to the data. (●) Infrared fluorescence measurements, (■) infrared absorption measurements at ca. 1900 cm^{-1} , (▲) infrared absorption measurements at ca. 1918 cm^{-1} .

[obtained after photolyzing $\text{Cr}(\text{CO})_6$ at 248 nm] shows broadening and a red shift of the $\nu_{\text{CO}}(\text{b}_2)$ band, consistent with the population of hot bands in the nascent species. Similar observations have been reported by Weitz and co-workers.^{17,26} If the CO laser is tuned to the red side of the b_2 band (ca. 1900 cm^{-1}), absorption is found to decay with time and also with increasing [He]. If the CO laser is tuned to the maximum absorption of 300K $\text{Cr}(\text{CO})_4$ (ca. 1919 cm^{-1}), absorption is observed to increase with time and with [He]. The decay at 1900 cm^{-1} , the gain at 1918 cm^{-1} , and the fluorescence decay all have the same [He] dependence within our experimental uncertainty.²⁷ See Figure 4. From these data, we find that $[\text{Cr}(\text{CO})_4]^*$ is stabilized by collisions with He, with a rate constant $k_s = 2.6 \pm 0.5 \times 10^5 \text{ Torr}^{-1} \text{ s}^{-1}$. This yields a value of $\beta \approx 0.01$, where $\beta = k_s/Z$. The addition of small amounts (ca. 0.40 Torr) of CO to $\text{Cr}(\text{CO})_6/\text{He}$ mixtures changes the stabilization rate by less than the experimental uncertainty in k_s . The value for k_s determined here is comparable to that found²⁸ for the stabilization of $[\text{Mn}(\text{CO})_5]^*$ by He. The stabilization rate for $[\text{Cr}(\text{CO})_4]^*$ due to collisions with $\text{Cr}(\text{CO})_6$ can be determined from the intercept of the line in Figure 4; $k_s^{\text{Cr}} = 2.5 \times 10^7 \text{ Torr}^{-1} \text{ s}^{-1}$. Thus, under our experimental conditions, $\sum k_s[\text{M}] \approx 2.6 \times 10^5 [\text{CO}] + 0.4 \times 10^6$ (units of s^{-1}). The similarity of the values of $k_s[\text{M}]$ for $[\text{Cr}(\text{CO})_4]^* + \text{He}$ and $[\text{Mn}(\text{CO})_5]^* + \text{He}$ suggest that our value of $\sum k_s[\text{M}]$ can serve as a useful approximation in the cases of $[\text{Cr}(\text{CO})_5]^*$ and $[\text{Cr}(\text{CO})_6]^*$ relaxation, as well.

The considerations outlined here permit us to evaluate the RRKM model for $k_a(E)$, eq 14, the chemical activation distribution function, eq 15, and the Hinshelwood-Lindemann expression for k_{obsd} , eq 13. Our approach is to calculate k_{obsd} versus pressure for several choices of E_0 . The calculations in best agreement with experimental data will indicate the best choice for E_0 . This procedure cannot yield precise data on E_0 due to uncertainties in the data and the various parameters required for the calculations. These parameters include the stabilization rate, k_s , the transition state's (and, in some cases, reactant's) vibrational frequencies, and moments of inertia. We have therefore varied all of these parameters to determine the sensitivity of k_{obsd} to them. This study was done for the reaction of $\text{Cr}(\text{CO})_4$ with CO (vide infra) because the quality of our experimental data was better in this case than for the analogous reaction of $\text{Cr}(\text{CO})_5$ with CO. In agreement with ref 25, we find that the values of $k_a(E)$ calculated with eq 14 for the dissociation of either $\text{Cr}(\text{CO})_6$ or $\text{Cr}(\text{CO})_5$ are, within 10%, constant with respect to variation of

(26) Seder, T. A.; Ouderkirk, A. J.; Weitz, E. *J. Chem. Phys.* **1986**, *85*, 1977.(27) The vibrational relaxation effects observed here are the origin of the biexponential decays observed for $[\text{Cr}(\text{CO})_4]$ at low [He]. See Experimental Section.(28) Bray, R. G.; Seidler, P. F.; Gethner, J. S.; Woodin, R. L. *J. Am. Chem. Soc.* **1986**, *108*, 1312.(23) Braterman, P. S. *Metal Carbonyl Spectra*; Academic: New York, 1975.(24) Waage, E. V.; Rabinovitch, B. S. *Chem. Rev.* **1970**, *70*, 377.(25) Astholz, D. C.; Troe, J.; Wieters, W. *J. Chem. Phys.* **1979**, *70*, 5107.

Table III. Metal Carbonyl Bond Dissociation Energies

compd	DH° (kcal/mol)	ref
Cr(CO) ₆	37	12, 13
Cr(CO) ₅	25	this work
Fe(CO) ₅	55.4	14
Fe(CO) ₄	4.6	14
Fe(CO) ₃	32.3	14
Ni(CO) ₄	25	15
Ni(CO) ₃	13	15
Ni(CO) ₂	54	15
[Mn(CO) ₅] ⁺	20.2	11
[Cr(CO) ₆] ⁺	34.4	31
[Cr(CO) ₅] ⁺	5.0	31
[Cr(CO) ₄] ⁺	19.1	31

reactant or transition-state frequencies, so long as ΔS^\ddagger is held constant. In both cases we use $\Delta S^\ddagger = 9.9$ eu since this is the experimentally determined value¹³ for Cr(CO)₆ and should also be an excellent approximation for Cr(CO)₅. This follows from the similarity¹³ of ΔS^\ddagger for the dissociation of Fe(CO)₅ and Cr(CO)₆ and also from thermochemical estimates²⁹ of ΔS^\ddagger . Variation in the value of k_s by $\pm 50\%$ produces a variation in k_{obsd} of ca. $\pm 10\%$, i.e., on the order of the experimental uncertainty. Error limits on E_0 determined here are estimated by holding all computational parameters, other than E_0 , fixed and visually comparing calculated and experimental $k_{\text{obsd}}[M]$ versus $[M]$ curves. This is a somewhat more conservative estimate than is obtained by, e.g., a χ^2 test.³⁰ Taking account of our experimental uncertainty in determining k_{obsd} , we conclude that values of E_0 determined as described here are accurate only to within ± 5 kcal/mol. The values of E_0 and DH° thus determined are nevertheless useful because, especially in the case of reactive intermediates such as Cr(CO)₅, conventional experimental techniques for determining E_0 or DH° are not generally applicable.

The pressure dependence of the rate constant for the recombination of Cr(CO)₅ with CO is shown in Figure 2. Data are compared with a RRKM calculation where $E_0 = 37$ kcal/mol. The quality of the data precludes a detailed comparison but calculation and experiment appear to be qualitatively in accord with one another. Note that experimental data are "fit" only by varying E_0 . All other parameters are fixed. The critical energy, E_0 , for the decomposition of Cr(CO)₆ is approximately equal to the bond dissociation energy, DH°[(CO)₅Cr-CO]. We conclude that DH°[(CO)₅Cr-CO] = 37 ± 5 kcal/mol. Peters and co-workers,¹² using the technique of photoacoustic calorimetry, find DH° ~ 37 kcal/mol, and similar conclusions were reached by Lewis et al.,¹³ using the method of laser powered homogeneous pyrolysis (LPHP). Our results are consistent with these reports.

The application of the RRKM method to the Cr(CO)₄ + CO recombination, i.e., the decomposition of [Cr(CO)₅]^{*}, is of particular interest as a means for estimating DH°[(CO)₄Cr-CO].

This is because techniques such as photoacoustic calorimetry and LPHP cannot easily be applied to reactive intermediates. Experimental data on the pressure dependence of the Cr(CO)₄ + CO recombination are compared with RRKM calculations in Figure 3. In these calculations, E_0 was varied (20–40 kcal/mole) while other parameters were held at the values listed in Table II. It is clear that a calculation with $E_0 \sim 25$ kcal/mol is consistent with the experimental data, while calculations where $E_0 = 20$ or 40 kcal/mol are not. These results thus indicate that DH°[(CO)₄Cr-CO] = 25 ± 5 kcal/mol.

The utility of this approach to evaluating DH° is determined, in part, by the sensitivity of the physical model to the selection of input parameters (Tables I and II). As previously discussed, the calculations are relatively insensitive to the choice of transition-state vibrational frequencies²³ so long as the values selected yield the "correct" ΔS^\ddagger . In the case of eq 2, an experimentally determined value for ΔS^\ddagger was used,¹³ while for eq 3, a value consistent with ΔS^\ddagger values for other metal carbonyls¹³ was assumed. In both cases, $\Delta S^\ddagger = 9.9$ eu. Variations in the value of the reaction path degeneracy, L^\ddagger , by $\pm 25\%$, or the effective value of the stabilization rate constant, k_s , by $\pm 50\%$ cause variations in k_{obsd} within our experimental uncertainty. We conclude that the Cr(CO)₅ bond dissociation energy is DH° = 25 ± 5 kcal/mol.

There has been no measurement of DH°[(CO)₄Cr-CO], other than the present one, reported. Comparisons with DH° values for other transition-metal carbonyls can be useful in assessing whether the DH° determined here is physically reasonable. Such values are listed in Table III. A trend is apparent, i.e., the second bond dissociation energy for the metal carbonyls listed is significantly lower than the first. Additionally, the bond dissociation energy of [Mn(CO)₅]⁺, a species isoelectronic and isostructural with Cr(CO)₅, is reported to be 20.2 kcal/mol. Both observations are consistent with our finding, DH°[(CO)₄Cr-CO] = 25 ± 5 kcal/mol.

Conclusions

Time resolved infrared laser absorption spectroscopy has been used to study the kinetics of the recombination of both Cr(CO)₄ and Cr(CO)₅ with CO. The observed recombination rate constants, k_{obsd} , are constant at high pressure but fall off with decreasing pressure. This behavior is interpreted in terms of a Hinshelwood-Lindemann type mechanism consisting of an association step (rate constant, k_c), a decomposition step (k_a) and a stabilization step ($\sum k_s[M]$). We determine k_c from the high pressure limiting rate constant for recombination and $\sum k_s[M]$ from both infrared fluorescence and time resolved line shape measurements. RRKM theory is used to compute $k_a(E)$ as a function of E_0 , the critical energy for the decomposition step. The resulting set of rate constants $\{k_c, \sum k_s[M] \text{ and } k_a(E)\}$ are used to compute k_{obsd} as a function of pressure, $[M]$. Comparison with experimental data then permits E_0 to be estimated. In this way, we can evaluate metal-ligand bond dissociation energies for both stable molecules, e.g. Cr(CO)₆, and coordinatively unsaturated reactive intermediates, such as Cr(CO)₅. Our results are; DH°[(CO)₄Cr-CO] = 37 ± 5 kcal/mol, in agreement with previous studies, and DH°[(CO)₄Cr-CO] = 25 ± 5 kcal/mol.

Acknowledgment is made to the National Science Foundation for support of this research through Grant CHE-8500713.

(29) Benson, S. W. *Thermochemical Kinetics*, 2nd ed.; Wiley-Interscience: New York, 1976; pp 90.

(30) Bevington, P. R. *Data Reduction and Error Analysis for the Physical Sciences*; McGraw-Hill: New York, 1969; pp 187.

(31) Bidinosti, D. R.; McIntyre, N. S. *Can. J. Chem.* 1967, 45, 641.